Linear dichroic x-ray absorption response of Ti-Ti dimers along the c axis in Ti₂O₃ upon Mg substitution

M. Okawa [1,*] D. Takegami [2] D. S. Christovam [2] M. Ferreira-Carvalho [2,3] C.-Y. Kuo [2,4,5] C. T. Chen,[5] T. Miyoshino,[1]
K. Takasu,[6] T. Okuda,[6] C. F. Chang [2] L. H. Tjeng [2] and T. Mizokawa [1,†]

[1]*Department of Applied Physics, Waseda University, Tokyo 169-8555, Japan*
[2]*Max Planck Institute for Chemical Physics of Solids, 01187 Dresden, Germany*
[3]*Institute of Physics II, University of Cologne, 50937 Cologne, Germany*
[4]*Department of Electrophysics, National Yang Ming Chiao Tung University, Hsinchu 30010, Taiwan*
[5]*National Synchrotron Radiation Research Center (NSRRC), Hsinchu 30076, Taiwan*
[6]*Graduate School of Science and Engineering, Kagoshima University, Kagoshima 890-0065, Japan*

Corundum oxide Ti₂O₃ shows the metal-insulator transition around 400–600 K accompanying the nearest Ti³⁺-Ti³⁺ bond ($a_{1g}a_{1g}$ singlet state) formation along the c axis. In order to clarify the hole-doping effect for the $a_{1g}a_{1g}$ singlet bond in Ti₂O₃, we investigated Ti $3d$ orbital anisotropy between corundum-type Ti₂O₃ and ilmenite-type MgTiO₃ using linear dichroism of soft x-ray absorption spectroscopy of the Ti $L_{2,3}$ edge. From the linear dichroic spectral weight in Mg$_y$Ti$_{2-y}$O₃, we confirmed that the $a_{1g}a_{1g}$ state is dominant not only in $y = 0.01$ (almost Ti₂O₃), but also in $y = 0.29$, indicating that the Ti-Ti bond survives against a certain level of hole doping. In $y = 0.63$ corresponding to 46% hole doping per Ti, the $3d$ orbital symmetry changes from a_{1g} to e_g^π.

I. INTRODUCTION

Orbital degrees of freedom frequently play an essential role in the electronic properties of transition-metal oxides [1]. The metal-insulator transitions in rutile-type VO₂, for example, are governed by the bond formation between the V $3d$ orbitals in the edge-sharing VO₆ octahedra [2]. There are also a variety of orbitally assisted bond formations in spinel and hollandite systems, which were studied theoretically [3,4] and experimentally [5–10]. Yet, in corundum-type V₂O₃, the bond formation surprisingly does not occur between the V ions in the face-sharing pairs of VO₆ octahedra along the c axis [11]. In contrast, Ti-Ti molecular orbital formation does occur in Ti₂O₃: The Ti-Ti distance of the pair is gradually shortened in going from 600 to 400 K, and Ti₂O₃ undergoes a metal-to-insulator transition (Fig. 1) [12–15]. As shown in Figs. 1(a) and 1(b), it has theoretically been shown that the Ti $3d$ a_{1g} orbitals form the molecular orbitals which build up the insulating state [16–21]. The theoretical predictions have been followed by the experimental confirmations by soft x-ray absorption spectroscopy (XAS) [22,23] and photoemission spectroscopy (PES) [23]. In addition to the corundum Ti₂O₃ with d^1 honeycomb layers coupled by the face-sharing TiO₆ pairs, MgVO₃, which is a novel ilmenite system with d^1 configuration, has been found to form V-V dimers in the d^1 honeycomb lattice below 500 K [24]. It is also known that

layered Ti trihalides such as TiCl₃ and TiBr₃ harbor the d^1 honeycomb lattice with Ti-Ti dimerization [25,26].

Very recently, the impact of Mg substitution for Ti in the Mg$_y$Ti$_{2-y}$O₃ system, which is also known as Mg$_{1-x}$Ti$_{1+x}$O₃ with $y = 1 - x$ (hereafter, we use the notation with y), has been studied by Takasu *et al.* [27]. While Ti₂O₃ is the well-studied corundum system, MgTiO₃ is an ilmenite system with Ti⁴⁺ (d^0) configuration. Therefore, Mg$_y$Ti$_{2-y}$O₃ provides a unique opportunity to study evolution from the face-sharing TiO₆ pairs in the d^1 corundum system to the d^0/d^1 mixed valence honeycomb lattice in the ilmenite. It is expected that the Ti $3d$ t_{2g} orbitals play essential roles to control their electronic properties. It has been revealed that the shortened Ti-Ti bonds survive against the hole doping by the Mg²⁺ substitution for Ti³⁺. Here, the interesting question arises whether the Ti $3d$ a_{1g} orbitals are still occupied in the hole-doped system to stabilize the Ti-Ti molecular orbitals.

As shown in the previous XAS studies [22,23], the particular linear dichroism (LD) of the Ti $2p$ spectrum between the polarization vector ($\boldsymbol{E}$) perpendicular to and parallel to the c axis played a vital role for clarifying the a_{1g} occupation in the Ti₂O₃ system. In the present work, we report LD-XAS of Mg$_y$Ti$_{2-y}$O₃ with $y = 0.01, 0.29, 0.63$, and 1.00 to clarify the hole-doping effect on the $a_{1g}a_{1g}$ singlet bond. Based on the experimental results, we discuss the interplay between orbital symmetry and hole doping.

II. EXPERIMENT AND CALCULATIONS

Single crystals of Mg$_y$Ti$_{2-y}$O₃ with $y = 0.01, 0.29, 0.63$, and 1.00 were grown using the floating-zone method, and

---

*Corresponding author: mokawa@aoni.waseda.jp
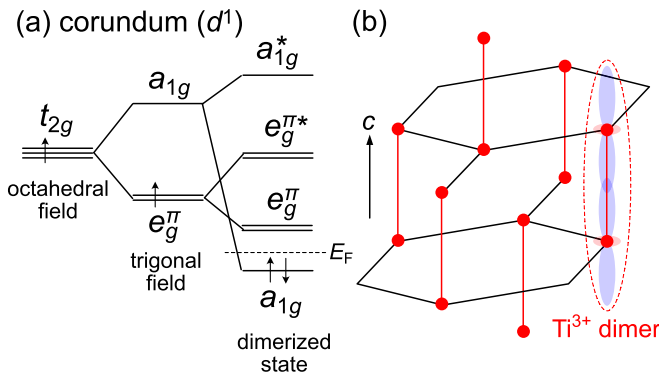†Corresponding author: mizokawa@waseda.jp

FIG. 1. (a) Energy diagram of the *d* orbitals in the corundum-type d^1 insulators with formation of d^1-d^1 singlet bond [21]. (b) The Ti-Ti bond formation between honeycomb layers along the *c* axis in Ti$_2$O$_3$. The shaded areas are a schematic of Ti 3*d* a_{1g} orbitals.

the compositions *y* were determined by the energy-dispersive x-ray spectroscopy, whose details were described in the literature by Takasu *et al.* [27]. The Ti ions in the octahedral coordination are substituted by the Mg ions. The single crystals were mounted on the sample holders *ex situ* after orientation by the single-crystal x-ray diffraction using a Rigaku R-AXIS RAPID II diffractometer. LD-XAS measurements with the total electron yield method were performed at the NSRRC-MPI TPS 45A1 Submicron Soft X-ray Spectroscopy Beamline [28] at Taiwan Photon Source, National Synchrotron Radiation Research Center (NSRRC). Clean sample surfaces were obtained by cleaving the crystals *in situ*, with the *c* axis nearly in-plane of the cleaved surface. LD-XAS data were acquired using a 98% horizontal linear polarized soft x-ray beam, at a geometry close to normal incidence. The LD spectra were obtained by first setting the sample stage to measure with the *c* axis aligned parallel to the polarization direction, and then rotating the stage in-plane 90° to obtain the geometry with the *c* axis aligned perpendicular to the polarization. The maximum dichroism at the chosen directions was verified to confirm the correct orientations. The sample temperature was 300 K for all measurements, and an overall energy resolution was ∼0.25 eV.

In order to extract information about the orbital occupation from the XAS spectra, we have made use of simulations utilizing the well-proven single-site TiO$_6$ and double-site Ti$_2$O$_9$ cluster-model calculations performed by Sato *et al.* [22] and by Chang *et al.* [23], respectively. The method includes the full atomic multiplet theory and the local effects of the solid. It accounts for the intra-atomic Ti 3*d*-Ti 3*d* and Ti 2*p*-Ti 3*d* Coulomb interactions, the atomic Ti 2*p* and Ti 3*d* spin-orbit couplings, the O 2*p*-Ti 3*d* hybridization, and the proper local crystal-field parameters [29].

III. RESULTS AND DISCUSSION

Figure 2(a) shows the linear polarization dependence of the Ti $L_{2,3}$ edges for each *y* composition. The energy regions of 454–461 and 461–467 eV can be assigned to the L_3 ($2p_{3/2} \rightarrow 3d$) and L_2 ($2p_{1/2} \rightarrow 3d$) absorption edges, respectively, although there is considerable overlap or mixing between the two edges [30,31]. In the compositions of *y* = 0.63 and 1.00,
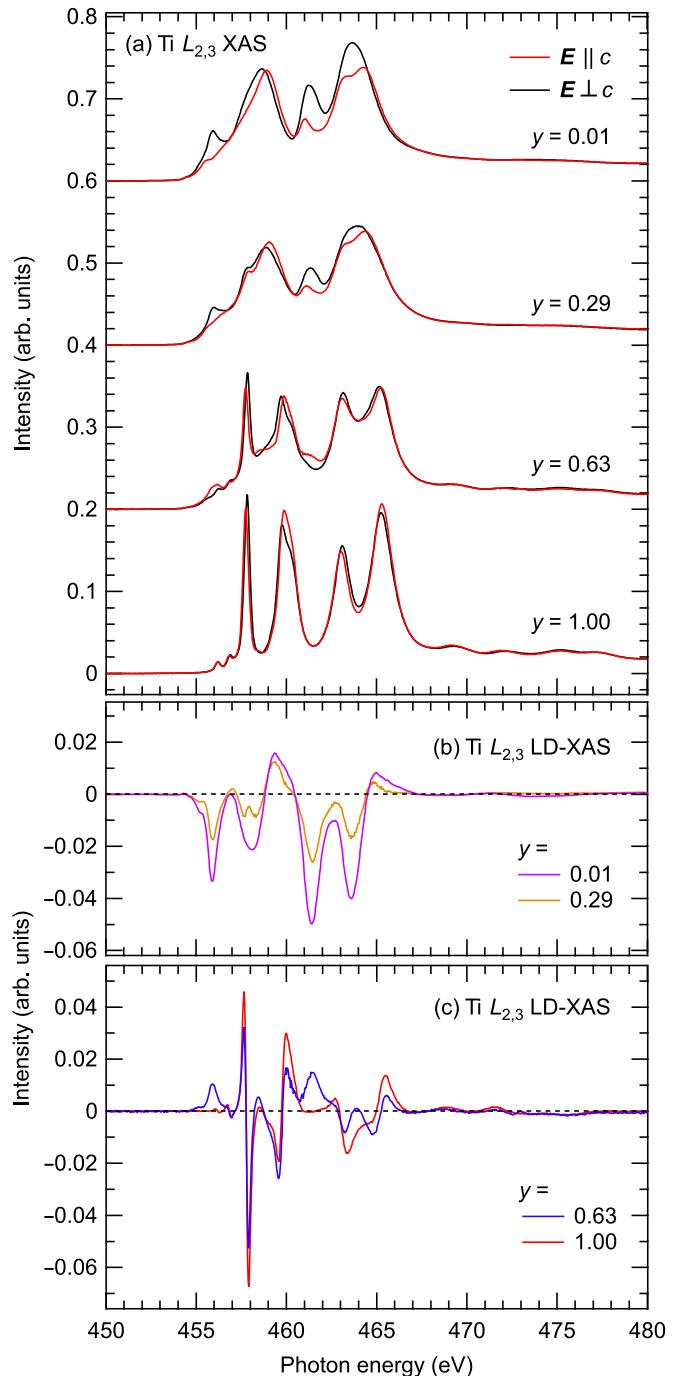

FIG. 2. (a) Ti $L_{2,3}$ XAS of Mg$_y$Ti$_{2-y}$O$_3$ for *y* = 0.01, 0.29, 0.63, and 1.00. The XAS intensities obtained with the linear-polarized direction of the incident beam (**E**) parallel to and perpendicular to the *c* axis correspond to red (**E** ∥ *c*) and black (**E** ⊥ *c*) curves, respectively. LD-XAS spectra obtained by the difference between the **E** ∥ *c* and **E** ⊥ *c* geometries were shown in (b) for *y* = 0.01 and 0.29, and in (c) for *y* = 0.83 and 1.00. Dashed lines correspond to zero LD intensity.

the sharp peaks at 458 and 460 eV are related (but not equal) to the octahedral crystal-field splitting at the Ti^{4+} sites [30]. Ti $L_{2,3}$ LD were obtained as spectral differences between **E** ∥ *c* and **E** ⊥ *c* geometries for each *y*, as shown in Fig. 2(b). In *y* = 0.01, which is almost Ti$_2$O$_3$ composition, the LD-XAS
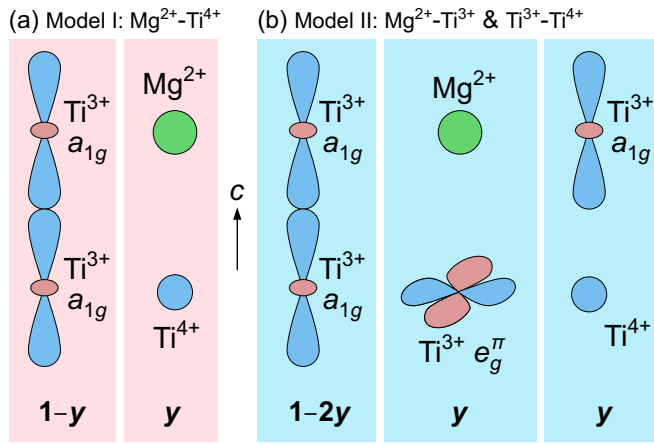
FIG. 3. (a) Model I, corresponding to a Ti^{3+}-Ti^{3+} pair with occupied a_{1g}-a_{1g} orbitals and Mg^{2+}-Ti^{4+} pairs with empty Mg $3s$ and Ti $3d$ orbitals. Their relative populations are $1-y$ and y, respectively. (b) Model II, corresponding to a Ti^{3+}-Ti^{3+} pair with occupied a_{1g}-a_{1g} orbitals, Mg^{2+}-Ti^{3+} pairs with empty Mg $3s$ and occupied Ti $3de_g^\pi$ orbitals, and Ti^{3+}-Ti^{4+} pairs with occupied Ti $3d$ a_{1g} and empty Ti $3d$ orbitals. Their relative populations are $1-2y$, y, and y, respectively.

spectrum is consistent with the previous reports of Ti_2O_3 at room temperature [22,23]. The LD features in $y = 0.01$ also appeared in the LD spectrum of $y = 0.29$ with a small Ti^{4+} component, which can be seen at 458 eV. In contrast to $y = 0.01$ and 0.29, Ti $L_{2,3}$ XAS spectra in heavily Mg-substituted $y = 0.63$ and $MgTiO_3$ ($y = 1.00$) have very different line shapes. They are dominated by the Ti^{4+} component, as we will show below.

In analyzing the LD spectrum of the $y = 0.29$ composition, we first tried to construct it from the LD spectra of the $y = 0.01$ and $y = 1.00$ compositions with weights that follow from the $y = 0.29$ value. This first model is illustrated in Fig. 3(a), where the $y = 0.01$ is represented by Ti^{3+}-Ti^{3+} pairs with occupied a_{1g}-a_{1g} $3d$ orbitals and the $y = 1.00$ by Mg^{2+}-Ti^{4+} pairs with empty Mg $3s$ and Ti $3d$ orbitals, respectively. We then obtained a sum of the LD of the $y = 0.01$ multiplied by $2(1 - 0.29)/(2 - 0.29) = 0.83$ and the LD of the $y = 1.00$ multiplied by $0.29/(2 - 0.29) = 0.17$, where we note that the factors $1/(2 - 0.29)$ account for the fact that the spectra in Fig. 2(a) with different Ti contents were normalized to the integrated intensity. The result is shown in Fig. 4(a) and clearly does not match the measured LD of the $y = 0.29$. The latter shows mainly the same LD of the $y = 0.01$, but reduced by about 50%, and very little of the LD of the $y = 1.00$.

This discrepancy let us to conclude that the substitution of Ti by Mg does not create Mg^{2+}-Ti^{4+} pairs, but rather Mg^{2+}-Ti^{3+} pairs with the Ti^{4+} being located somewhere else and thus forming Ti^{3+}-Ti^{4+} pairs. This conclusion is consistent with the findings of a recent photoemission study which revealed that the holes introduced by the Mg substitution are in the Ti-Ti pairs [32]. We thus arrive at the second model as depicted in Fig. 3(b): the $y = 0.29$ material is composed of Mg^{2+}-Ti^{3+} pairs, with the empty Mg $3s$ orbital and the singly occupied Ti $3d$ orbital (of the e_g^π type, as we will show later), Ti^{3+}-Ti^{4+} pairs with the singly occupied $3d$ orbital (of the a_{1g} type) and the fully unoccupied $3d$ orbitals, respectively,
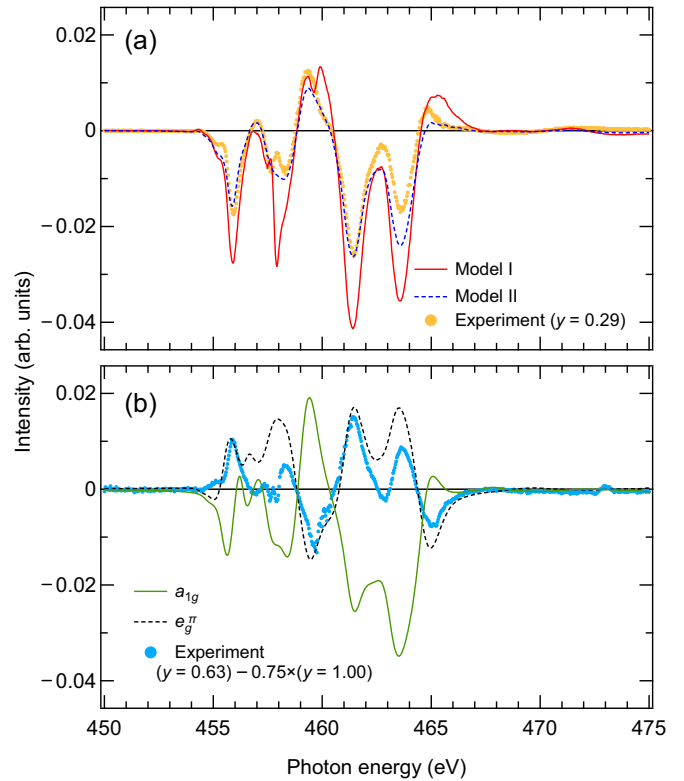

FIG. 4. (a) Calculated LD spectra for $y = 0.29$ using the relative populations of the Ti sites corresponding to models I (red solid curve) and II (blue broken curve), as defined in Figs. 3(a) and 3(b), respectively, and further elaborated in the text, together with the experimental LD (yellow dots). For model I, the calculations for the double-site $Ti_2^{3+}O_9$ cluster are adapted from the work performed by Chang *et al.* [23]. For model II, the calculations for the single-site $Ti^{3+}O_6$ cluster are reproduced with permission from Ref. [22]. (b) LD spectra of the Ti^{3+} ions (blue dots), obtained from the difference between the LD intensities of $I_{LD}(y = 0.63)$ and $0.75 \times I_{LD}(y = 1.00)$, compared to the TiO_6 cluster-model calculations assuming the a_{1g} (green solid curve) or e_g^π (black broken curve) orbital occupied. Here we finely aligned the $I_{LD}(y = 1.00)$ by shifting it 8 meV to prevent derivative artifacts from the Ti^{4+} contributions.

and Ti^{3+}-Ti^{3+} pairs with a_{1g}-a_{1g}. The relative weights of the components are also indicated, namely, y, y, and $1-2y$, respectively. The LD spectra of the Ti^{3+} ions in the Mg^{2+}-Ti^{3+} and Ti^{3+}-Ti^{4+} pairs can be estimated from the earlier TiO_6 cluster calculations [22,23], as also shown in Fig. 4(b). Making the sum of the LD spectra from an e_g^π Ti^{3+} and an a_{1g} Ti^{3+} cluster plus the LD from the $y = 0.01$ with 0.29, 0.29, and $2(1 - 2 \times 0.29)$ weights, respectively, followed by the $1/(2 - 0.29)$ multiplication, we obtain a result that is very close to the experimental LD of $y = 0.29$ as displayed in Fig. 4(a). We note that assuming the Ti^{3+} in the Mg^{2+}-Ti^{3+} and Ti^{3+}-Ti^{4+} pairs are all e_g^π or all a_{1g} gives less satisfactory results.

Focusing now on the $y = 0.63$ composition, we observe that the sharpest features of the LD spectrum are given by those of the $y = 1.00$, i.e., by the Ti^{4+} in the Mg^{2+}-Ti^{4+} pairs. The LD spectra of the $y = 0.63$ and $y = 1.00$ are, however, not identical and the difference between them contains
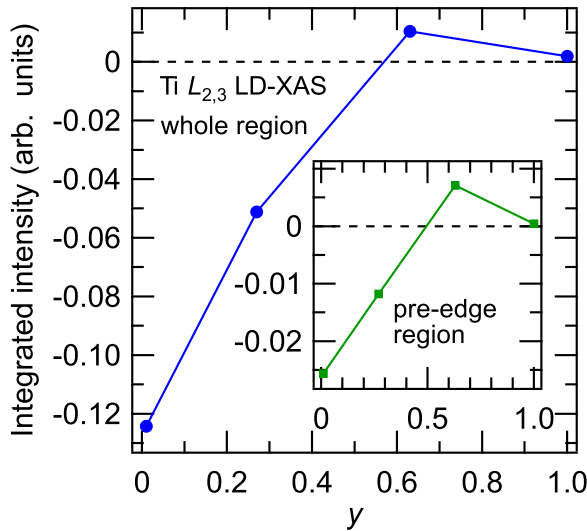
FIG. 5. Whole integrated intensity (450–470 eV) of Ti $L_{2,3}$ LD-XAS as a function of y in Mg$_y$Ti$_{2-y}$O$_3$. Inset: The integrated intensity around the pre-edge region (455–457 eV). The negative values in $y = 0.01$ and 0.29 [i.e., $I_{LD}(\boldsymbol{E} \parallel c) < I_{LD}(\boldsymbol{E} \perp c)$] mean dominating the Ti-Ti singlet bonds. The sign change from negative to positive at $y = 0.63$ mainly corresponds to the peaks at 456 and 462 eV, shown in Fig. 2(c).

information about the orbital state of the Ti^{3+} in the Mg^{2+}-Ti^{3+} and Ti^{3+}-Ti^{4+} pairs. Figure 4(b) shows this difference spectrum by the dotted curve. We can observe spectral features that matches well with those of the e_g^π in the TiO$_6$ cluster, e.g., the peaks at 455, 459.5, 461.5, 462.5, 463.5, and 465 eV. This supports our conjecture from the $y = 0.29$ composition in that the Ti^{3+} in the Mg^{2+}-Ti^{3+} pair is of the e_g^π type. At the same time, we now also see that in this high-Mg-content $y = 0.63$ composition, the Ti^{3+} of the Ti^{3+}-Ti^{4+} pairs are partly converted from a_{1g} to e_g^π.

To confirm our findings, we also analyzed the integrated intensities of the spectra and their polarization dependence since the use of sum rules gives direct information about the orbital polarization of the ground state [33,34]. Figure 5 shows the integrated intensity of the Ti $L_{2,3}$ LD-XAS spectra for the whole energy region (450–470 eV) and pre-edge region (455–457 eV). In $y \leqslant 0.29$ samples, integrated LD-XAS intensities are negative, i.e., $I(\boldsymbol{E} \parallel c) < I(\boldsymbol{E} \perp c)$. The a_{1g} orbital spreads along the c axis, while the e_g^π orbitals spread in the a-b plane, and thus the negative LD-XAS intensity can be expected by the relatively dominant a_{1g} orbital occupancy, suggesting that the Ti-Ti bonds along the c axis are still robust in $y = 0.29$. On the other hand, in $y = 1.00$ (MgTiO$_3$), the integrated Ti $L_{2,3}$ LD-XAS intensity is almost zero. This is consistent with the Ti^{4+} d^0 configuration, where all the t_{2g} and e_g orbitals are unoccupied. As for $y = 0.63$, the integrated value of Ti $L_{2,3}$ LD-XAS is positive, i.e., $I(\boldsymbol{E} \parallel c) > I(\boldsymbol{E} \perp c)$. The positive integrated value is mainly due to the positive LD signals at 456 eV (Ti L_3 pre-edge region) and at 462 eV (Ti L_2 pre-edge region), which are not observed for $y = 1.00$ in Fig. 2(b). As shown in the inset of Fig. 5, the LD signal of the Ti L_3 pre-edge region changes from negative to positive in going from $y = 0.29$ to $y = 0.63$. The sign change of the LD signal indicates that symmetry of the unoccupied Ti 3d

orbitals changes between $y = 0.29$ and $y = 0.63$. In $y = 0.63$, the a_{1g} orbital is less occupied and the e_g^π orbitals are more occupied than at $y = 0.29$; thus, the $\boldsymbol{E} \parallel c$ intensity is enhanced by the unoccupied a_{1g} state [Fig. 1(a)]. Therefore, the Ti-Ti bonds along the c axis tend to collapse at the hole-doping level for $y = 0.63$.

The Ti 3d orbital occupation changes from a_{1g} to e_g^π with the Mg doping. Since the e_g^π orbitals are extended along the Ti-Ti bonds in the honeycomb lattice layers, the e_g^π electrons can hop in the honeycomb lattice in the $y = 0.63$ system. Without dimerization, the $y = 0.63$ system is expected to be more metallic than the $y = 0.29$ system. On the other hand, while the a_{1g} orbital stabilizes the Ti-Ti bond in the face-sharing TiO$_6$ pairs, the e_g^π orbital may favor Ti-Ti dimers in the honeycomb lattice layer, as observed in MgVO$_3$. It would be interesting to study the $y = 0.63$ system using extended x-ray absorption fine structure (EXAFS) or pair-distribution function (PDF) experiments in order to detect local Ti-Ti dimers in the honeycomb lattice.

IV. CONCLUSION

We investigated the Mg^{2+} substitution effect to the Ti-Ti bonds along the c axis in Ti$_2$O$_3$ using LD-XAS measurements.

We found that the substitution of Ti by Mg does not lead to the formation of Mg^{2+}-Ti^{4+} pairs as previously thought. Instead, it creates Mg^{2+}-Ti^{3+} pairs, with the Ti^{4+} ions forming Ti^{3+}-Ti^{4+} pairs elsewhere in the structure. This conclusion was further supported by the observation that the holes introduced by the Mg substitution were found to be in the Ti-Ti pairs. We established a model for the $y = 0.29$ composition, which consists of Mg^{2+}-Ti^{3+} pairs with e_g^π orbital symmetry, Ti^{3+}-Ti^{4+} pairs with a_{1g} orbital symmetry, and Ti^{3+}-Ti^{3+} pairs with a_{1g}-a_{1g} singlet bonds. As the Mg content increased in the $y = 0.63$ composition, we observed a change in the orbital symmetry of the Ti^{3+} ions in the Ti^{3+}-Ti^{4+} pairs, with some converting from a_{1g} to e_g^π. The Ti-Ti bonds along the c axis tend to collapse at this hole-doping level for $y = 0.63$, indicating a significant impact of hole doping on the electronic properties. These findings in Mg$_y$Ti$_{2-y}$O$_3$ provide valuable insights into the electronic properties of transition-metal oxides and their metal-insulator transitions.

[1] D. I. Khomskii, *Transition Metal Compounds* (Cambridge University Press, Cambridge, 2014).

[2] M. W. Haverkort, Z. Hu, A. Tanaka, W. Reichelt, S. V. Streltsov, M. A. Korotin, V. I. Anisimov, H. H. Hsieh, H.-J. Lin, C. T. Chen, D. I. Khomskii, and L. H. Tjeng, Orbital-assisted metal-insulator transition in VO$_2$, Phys. Rev. Lett. **95**, 196404 (2005).

[3] D. I. Khomskii and T. Mizokawa, Orbitally induced peierls state in spinels, Phys. Rev. Lett. **94**, 156402 (2005).

[4] D. I. Khomskii and S. V. Streltsov, Orbital effects in solids: Basics, recent progress, and opportunities, Chem. Rev. **121**, 2992 (2021).

[5] M. Isobe and Y. Ueda, Observation of phase transition from metal to spin-singlet insulator in MgTi$_2$O$_4$ with $S = 1/2$ pyrochlore lattice, J. Phys. Soc. Jpn. **71**, 1848 (2002).

[6] M. Schmidt, W. Ratcliff, P. G. Radaelli, K. Refson, N. M. Harrison, and S. W. Cheong, Spin singlet formation in MgTi$_2$O$_4$: Evidence of a helical dimerization pattern, Phys. Rev. Lett. **92**, 056402 (2004).

[7] H. D. Zhou and J. B. Goodenough, Semiconductor-semiconductor transition in Mg[Ti$_2$]O$_4$, Phys. Rev. B **72**, 045118 (2005).

[8] M. Isobe, S. Koishi, N. Kouno, J.-I. Yamaura, T. Yamauchi, H. Ueda, H. Gotou, T. Yagi, and Y. Ueda, Observation of metal-insulator transition in hollandite vanadate, K$_2$V$_8$O$_{16}$, J. Phys. Soc. Jpn. **75**, 073801 (2006).

[9] Y. Ishige, T. Sudayama, Y. Wakisaka, T. Mizokawa, H. Wadati, G. A. Sawatzky, T. Z. Regier, M. Isobe, and Y. Ueda, Interplay between Mott physics and Peierls physics in hollandite-type vanadates with a metal-insulator transition, Phys. Rev. B **83**, 125112 (2011).

[10] T. Yamaguchi, M. Okawa, H. Wadati, T. Z. Regier, T. Saitoh, Y. Takagi, A. Yasui, M. Isobe, Y. Ueda, and T. Mizokawa, Electronic structure of spinel-type MgTi$_2$O$_4$: Valence change at surface and effect of Fe substitution for Mg, J. Phys. Soc. Jpn. **91**, 074704 (2022).

[11] J.-H. Park, L. H. Tjeng, A. Tanaka, J. W. Allen, C. T. Chen, P. Metcalf, J. M. Honig, F. M. F. de Groot, and G. A. Sawatzky, Spin and orbital occupation and phase transitions in V$_2$O$_3$, Phys. Rev. B **61**, 11506 (2000).

[12] F. J. Morin, Oxides which show a metal-to-insulator transition at the Neel temperature, Phys. Rev. Lett. **3**, 34 (1959).

[13] L. L. Van Zandt, J. M. Honig, and J. B. Goodenough, Resistivity and magnetic order in Ti$_2$O$_3$, J. Appl. Phys. **39**, 594 (1968).

[14] W. R. Robinson, The crystal structures of Ti$_2$O$_3$, a semiconductor, and (Ti$_{0.900}$V$_{0.100}$)$_2$O$_3$, a semimetal, J. Solid State Chem. **9**, 255 (1974).

[15] C. E. Rice and W. R. Robinson, High-temperature crystal chemistry of Ti$_2$O$_3$: Structural changes accompanying the semiconductor-metal transition, Acta Crystallogr. B **33**, 1342 (1977).

[16] H. J. Zeiger, Unified model of the insulator-metal transition in Ti$_2$O$_3$ and the high-temperature transitions in V$_2$O$_3$, Phys. Rev. B **11**, 5132 (1975).

[17] L. F. Mattheiss, Electronic structure of rhombohedral Ti$_2$O$_3$, J. Phys.: Condens. Matter **8**, 5987 (1996).

[18] A. Tanaka, On the metal-insulator transitions in VO$_2$ and Ti$_2$O$_3$ from a unified viewpoint, J. Phys. Soc. Jpn. **73**, 152 (2004).

[19] A. I. Poteryaev, A. I. Lichtenstein, and G. Kotliar, Nonlocal coulomb interactions and metal-insulator transition in Ti$_2$O$_3$: A cluster LDA + DMFT approach, Phys. Rev. Lett. **93**, 086401 (2004).

[20] V. Eyert, U. Schwingenschlögl, and U. Eckern, Covalent bonding and hybridization effects in the corundum-type transition-metal oxides V$_2$O$_3$ and Ti$_2$O$_3$, Europhys. Lett. **70**, 782 (2005).

[21] C. Castellani, C. R. Natoli, and J. Ranninger, Magnetic structure of V$_2$O$_3$ in the insulating phase, Phys. Rev. B **18**, 4945 (1978).

[22] H. Sato, A. Tanaka, M. Sawada, F. Iga, K. Tsuji, M. Tsubota, M. Takemura, K. Yaji, M. Nagira, A. Kimura, T. Takabatake, H. Namatame, and M. Taniguchi, Ti 3d orbital change across metal-insulator transition in Ti$_2$O$_3$: Polarization-dependent soft x-ray absorption spectroscopy at Ti 2p edge, J. Phys. Soc. Jpn. **75**, 053702 (2006).

[23] C. F. Chang, T. C. Koethe, Z. Hu, J. Weinen, S. Agrestini, L. Zhao, J. Gegner, H. Ott, G. Panaccione, H. Wu, M. W. Haverkort, H. Roth, A. C. Komarek, F. Offi, G. Monaco, Y.-F. Liao, K.-D. Tsuei, H.-J. Lin, C. T. Chen, A. Tanaka *et al.*, c-axis dimer and its electronic breakup: The insulator-to-metal transition in Ti$_2$O$_3$, Phys. Rev. X **8**, 021004 (2018).

[24] H. Yamamoto, S. Kamiyama, I. Yamada, and H. Kimura, Cation dimerization in a 3d^1 honeycomb lattice system, J. Am. Chem. Soc. **144**, 1082 (2022).

[25] S. Ogawa, Magnetic transition in TiCl$_3$, J. Phys. Soc. Jpn. **15**, 1901 (1960).

[26] S. Pei, J. Tang, C. Liu, J.-W. Mei, Z. Guo, B. Lyu, N. Zhang, Q. Huang, D. Yu, L. Huang, J. Lin, L. Wang, and M. Huang, Orbital-fluctuation freezing and magnetic-nonmagnetic phase transition in α-TiBr$_3$, Appl. Phys. Lett. **117**, 133103 (2020).

[27] K. Takasu, M. Arizono, T. Shirasaki, H. Arai, H. Kuwahara, T. Yoshida, T. Katsufuji, and T. Okuda, Crystal growth and magnetic properties of the MgTiO$_3$-Ti$_2$O$_3$ system, JPS Conf. Proc. **38**, 011116 (2023).

[28] H.-M. Tsai, H.-W. Fu, C.-Y. Kuo, L.-J. Huang, C.-S. Lee, C.-Y. Hua, K.-Y. Kao, H.-J. Lin, H.-S. Fung, S.-C. Chung, C.-F. Chang, A. Chainani, L. H. Tjeng, and C.-T. Chen, A submicron soft x-ray active grating monochromator beamline for ultra-high resolution angle-resolved photoemission spectroscopy, AIP Conf. Proc. **2054**, 060047 (2019).

[29] The parameters used in the TiO$_6$ cluster, in eV, are the following [23]: $U_{dd} = 4.0$, $U_{pd} = 5.5$, $\Delta = 6.5$, $10Dq_{ionic} = 0.85$, $V_{eg}^{\sigma} = 3.5$, $V_{eg}^{\pi} = 1.2$, $V_{a1g}^{\pi} = 0.9$. $\Delta_{trg} = -0.16$ and 0.16 for the e_g^{π} initial state and a_{1g} initial state calculations, respectively. The Ti$_2$O$_9$ clusters use the same parameters, with the addition of the Ti-Ti hopping integral V$_{dd\sigma} = 0.9$.

[30] F. M. F. de Groot, J. C. Fuggle, B. T. Thole, and G. A. Sawatzky, $L_{2,3}$ x-ray-absorption edges of d^0 compounds: K$^+$, Ca^{2+}, Sc^{3+}, and Ti^{4+} in O_h (octahedral) symmetry, Phys. Rev. B **41**, 928 (1990).

[31] F. M. F. de Groot, J. C. Fuggle, B. T. Thole, and G. A. Sawatzky, 2p x-ray absorption of 3D transition-metal compounds: An atomic multiplet description including the crystal field, Phys. Rev. B **42**, 5459 (1990).

[32] T. Miyoshino, D. Takegami, A. Meléndez-Sans, R. Nakamura, M. Yoshimura, K.-D. Tsuei, K. Takasu, T. Okuda, L. H. Tjeng, and T. Mizokawa, Intra *c*-axis dimer hybridization and mixed valency in Mg-doped Ti_2O_3, Phys. Rev. B **107**, 115145 (2023).

[33] S. I. Csiszar, M. W. Haverkort, Z. Hu, A. Tanaka, H. H. Hsieh, H.-J. Lin, C. T. Chen, T. Hibma, and L. H. Tjeng, Controlling orbital moment and spin orientation in CoO layers by strain, Phys. Rev. Lett. **95**, 187205 (2005).

[34] M. W. Haverkort, Spin and orbital degrees of freedom in transition metal oxides and oxide thin films studied by soft x-ray absorption spectroscopy, Ph.D. thesis, University of Cologne, 2005.